Bioorganic Chemistry 86 (2019) 598–608

Contents lists available at ScienceDirect

Bioorganic Chemistry

journal homepage: www.elsevier.com/locate/bioorg

Design and synthesis of new substituted spirooxindoles as potential inhibitors of the MDM2–p53 interaction

Assem Barakat[a,b,*], Mohammad Shahidul Islam[a], Hussien Mansur Ghawas[a], Abdullah Mohammed Al-Majid[a], Fardous F. El-Senduny[c], Farid A. Badria[d], Yaseen A.M.M. Elshaier[e], Hazem A. Ghabbour[f]

[a] Department of Chemistry, College of Science, King Saud University, P.O. Box 2455, Riyadh 11451, Saudi Arabia
[b] Department of Chemistry, Faculty of Science, Alexandria University, P.O. Box 426, Ibrahimia, Alexandria 21321, Egypt
[c] Department of Chemistry, Faculty of Science, Mansura University, Mansura, Egypt
[d] Department of Pharmacognosy, Faculty of Pharmacy, Mansoura University, Mansoura 35516, Egypt
[e] Department of Organic and Medicinal Chemistry, Faculty of Pharmacy, University of Sadat City, Menoufiya 32958, Egypt
[f] Department of Medicinal Chemistry, Faculty of Pharmacy, University of Mansoura, Mansoura 35516, Egypt

ARTICLE INFO

Keywords:
Spirooxindole
HCT-116
HepG2
PC-3
MDM2-p53
Protein–protein interaction

ABSTRACT

The designed compounds, **4a–p,** were synthesized using a simple and smooth method with an asymmetric 1,3-dipolar reaction as the key step. The chemical structures for all synthesized compounds were elucidated and confirmed by spectral analysis. The molecular complexity and the absolute stereochemistry of **4b** and **4e** designed analogs were determined by X-ray crystallographic analysis. The anticancer activities of the synthesized compounds were tested against colon (HCT-116), prostate (PC-3), and hepatocellular (HepG-2) cancer cell lines. Molecular modeling revealed that the compound **4d** binds through hydrophobic–hydrophobic interactions with the essential amino acids (LEU: 57, GLY: 58, ILE: 61, and HIS: 96) in the p53-binding cleft, as a standard p53-MDM2 inhibitor (**6SJ**). The mechanism underlying the anticancer activity of compound **4d** was further evaluated, and the study showed that compound **4d** inhibited colony formation, cell migration, arrested cancer cell growth at G2/M, and induced apoptosis through intrinsic and extrinsic pathways. Transactivation of p53 was confirmed by flow cytometry, where compound **4d** increased the level of activated p53 and induced mRNA levels of cell cycle inhibitor, *p21*.

1. Introduction

Cancer is a global health problem and is considered as the second cause of death after heart disease [1]. Cancer is a major cause of morbidity and mortality, with approximately 1,735,350 new cases in United States and 609,640 cancer-related deaths predicted by the end of 2018, affecting both sexes [1,2].

Many chemotherapeutic drugs are commercially available and several others are in clinical trials. However, several serious side effects are produced during treatment with these drugs, such as lymphedema, bone marrow depression, nephrotoxicity, alopecia, weakening of the immune system, which may result in infections and osteoporosis owing to their non-selective action. Another problem is that despite cytotoxic effects *in vitro* and tumor growth inhibition *in vivo*, additional complications may arise due to the existence of a small subtype of cells called cancer stem cells (CSCs). These cells are relatively resistant to therapy and are able to effect cancer cell repopulation *in vivo* after cytotoxic drug treatments have ended [2].

The tumor suppressor, p53 protein, plays an important role in the cell by preventing the division of cells carrying mutated versions of the genome. Under stress, hypoxia or DNA damage, p53 is translocated from the cytoplasm to the nucleus where it activates many genes required for DNA repair. If DNA damage is severe, p53 induces the expression of apoptotic proteins. Mutated p53 in many solid tumors has been linked to poor prognosis because functional p53 prevents the growth of cancer cells and their metastasis, in part, by downregulating the expression of metalloproteases [3]. The p53 level in cells is controlled by murine double minute 2 (MDM2) at different levels; via the ubiquitination of p53, followed by proteasomal degradation (ubiquitin-proteasome machinery), the inhibition of transcriptional activation of p53 via the induction of p53 export to the cytoplasm, and the attenuation of p53 binding to its target DNA sequence. Activated p53

* Corresponding author at: Department of Chemistry, College of Science, King Saud University, P.O. Box 2455, Riyadh 11451, Saudi Arabia.
E-mail address: ambarakat@ksu.edu.sa (A. Barakat).

https://doi.org/10.1016/j.bioorg.2019.01.053
Received 23 November 2018; Received in revised form 26 December 2018; Accepted 25 January 2019
Available online 31 January 2019
0045-2068/

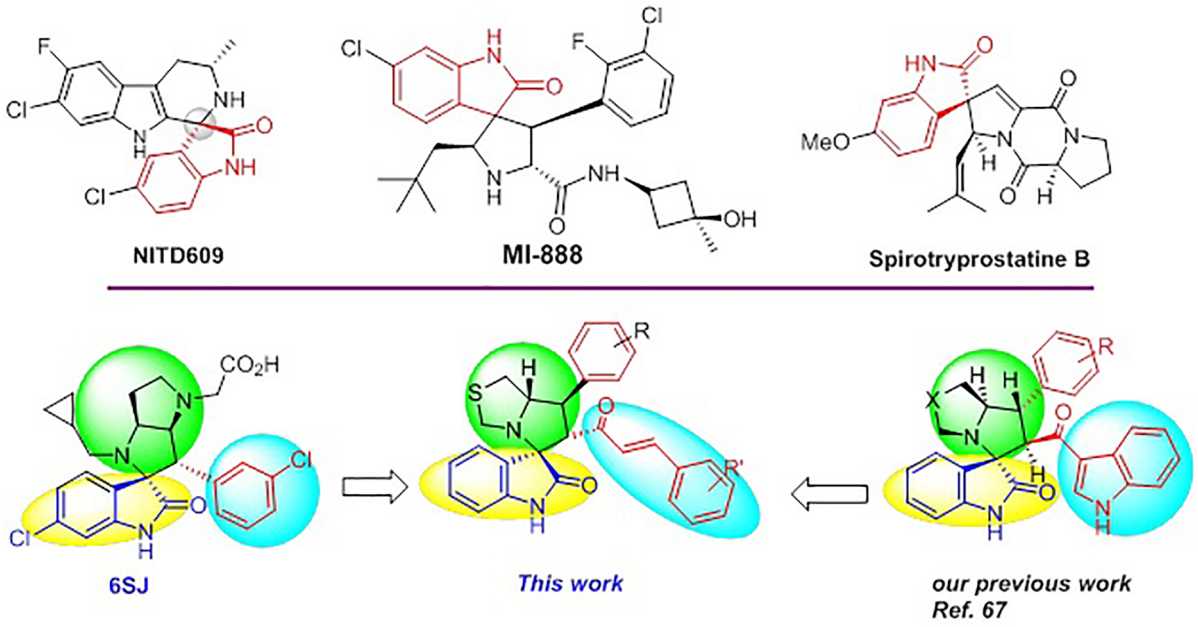

Fig. 1. Representative examples of spirooxindoles and our strategy for designing new analogs.

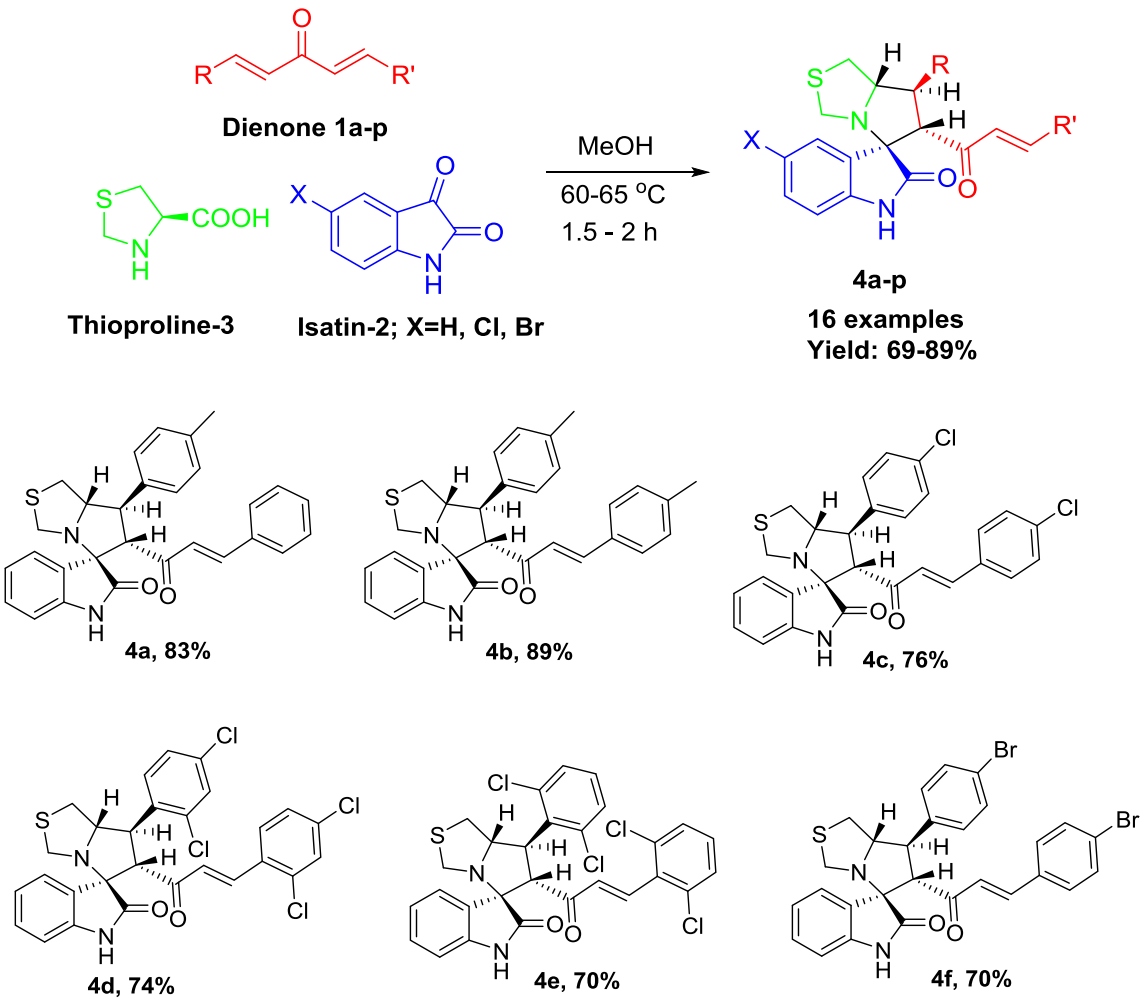

Scheme 1. The synthesized compounds, **4a–p**. The stereo-chemical outcome of the three-component reaction confirmed by X-ray single crystal techniques.

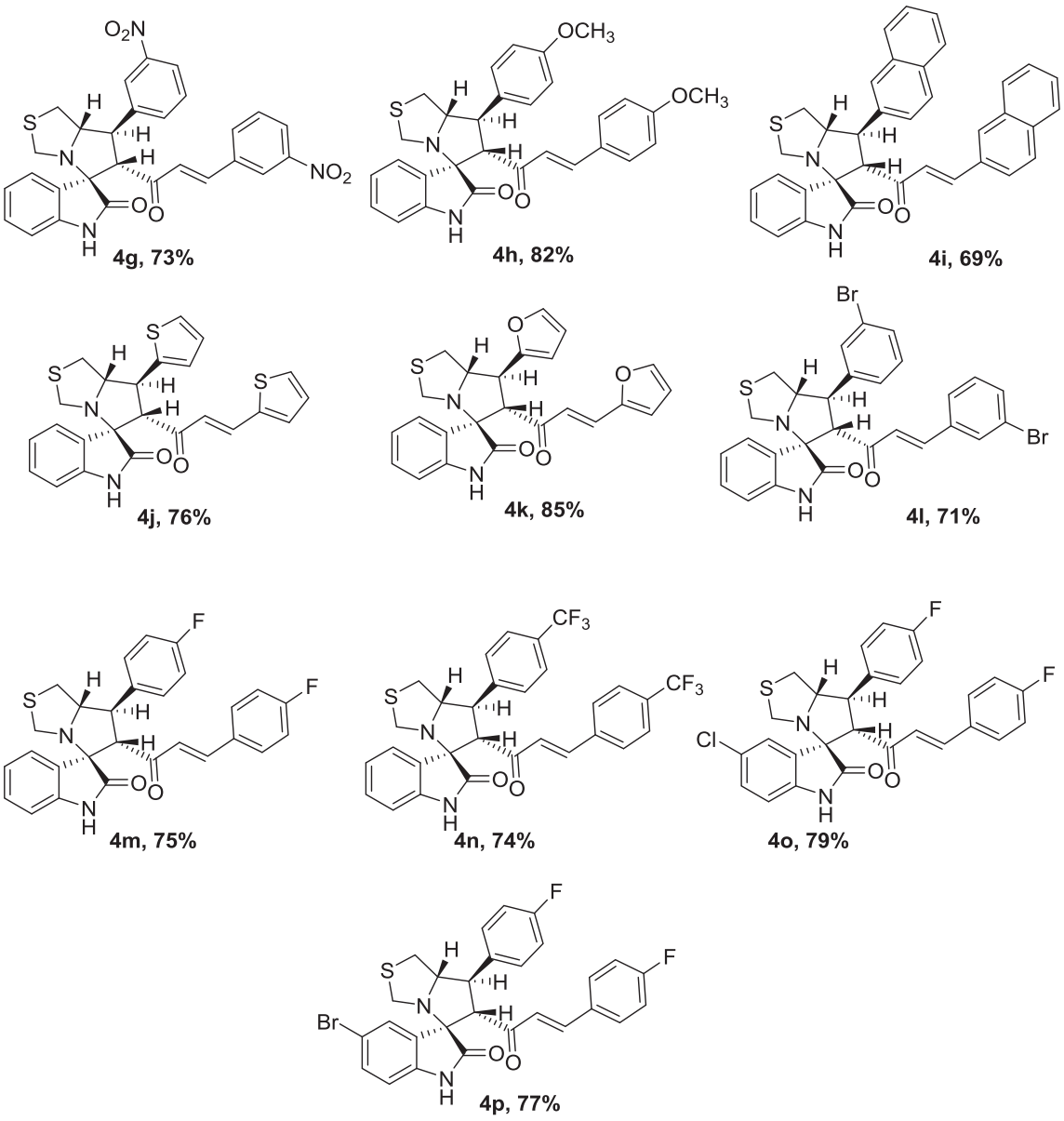

Scheme 1. (*continued*)

leads to the overexpression of its negative regulator, MDM2, therefore, it is considered as an autoregulatory loop [4–6].

Overexpression of MDM2 has been found in several types of cancers, including breast (5–40%), brain (11%), soft tissue tumors (17%) [7–10] and leukemia [11]. One of our pharmacological interests is to develop efficacious and safe agents for cancer therapy. Our approach is to synthesize small molecules which will be able to block the MDM2–p53 interaction and p53 reactivation [12–14]. Blocking of the MDM2–p53 protein–protein interaction and p53 activation have been previously reported using several selective small-molecule inhibitors [15–19]. Among 20 different chemical classes of compounds, three series are of particular importance: benzodiazepinediones, spirooxindoles and cis-imidazolines [8,19]. The diverse pharmacological activities and structures of spirooxindole frameworks have made them privileged unique structures in new drug discovery [20,21]. Some spirooxindoles were reported as specific small inhibitors, potent for MDM2–p53 protein–-protein interaction and p53 reactivation in cancer cells [15,16,18,19,22,23], such as, MI-888 and its derivatives (e.g. MI-219), which are extensively studied (*in vitro* and *ex vivo*) in preclinical stages [6,12,24], and **6SJ** (Fig. 1). Moreover, NITD609 is currently in clinical trials as an antimalarial drug [25,26].

Other types of natural oxindole alkaloids could be isolated, exemplified by spirooxindoles, like spirotryprostatins A and B (Fig. 1), which also show excellent anticancer activities [27]. Additionally, spirooxindole-containing compounds have been reported as inhibitors of tubulin [28] and actin [29] polymerization. All these have inspired more medicinal chemists to design analogs to study SARs and their modes of action [19,22,30–33]. The 1,3-cycloaddition of carbonyl compounds and amino acids to generate azomethine ylides, a powerful synthon in organic synthesis, subsequently reacting with dienophile to access pyrrolidine scaffolds, is important for biological activity [34]. This approach has been widely used to access spirooxindole scaffolds by different research groups [35–43].

Here, in continuation to our previous work and consideration of the aforementioned information, we have synthesized a new spirooxindole-based framework. The skeleton is constructed from scaffolds; (1) spirooxindole moiety, (2) thiazolo-pyrrolidine system, (3) 3-cinnamoyl derivatives, and (4) aryl ring at α-position to cinnamoyl ring (Fig. 1).

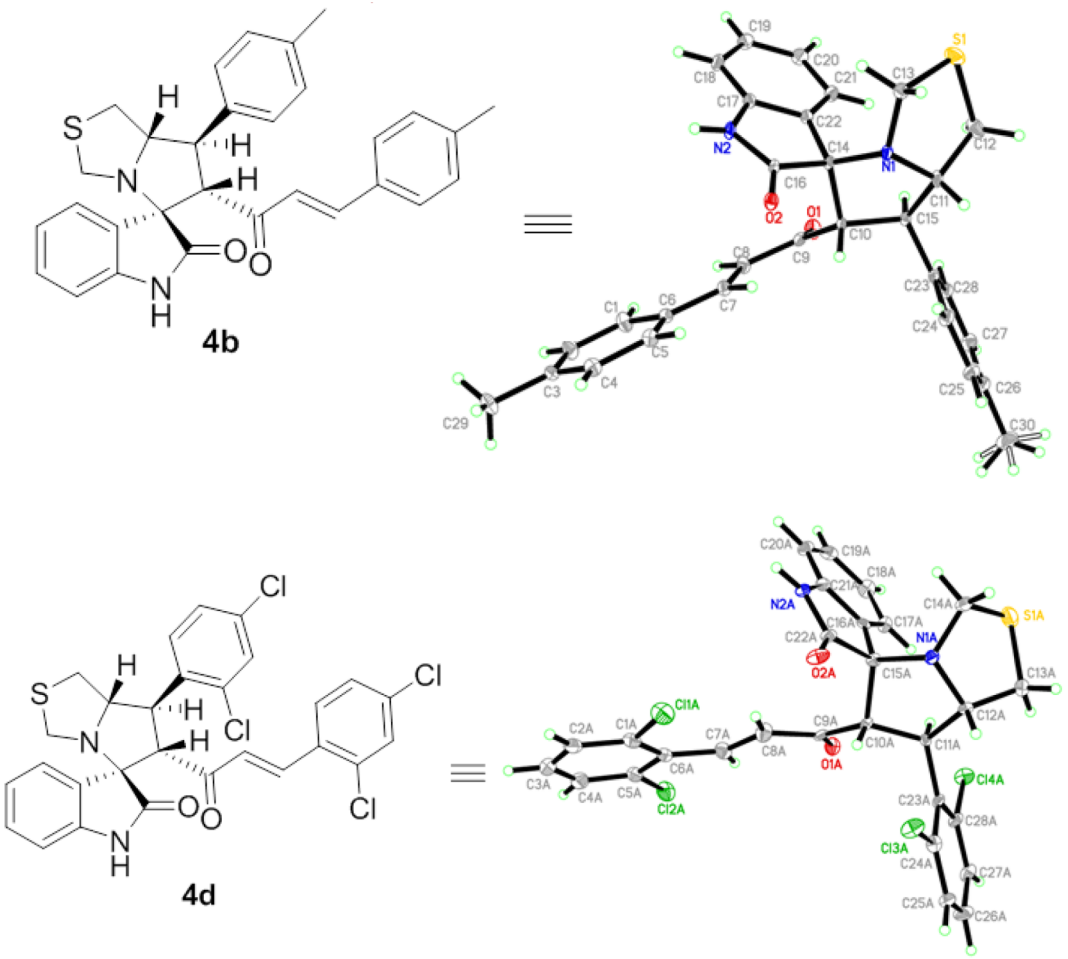

Fig. 2. Relative configuration from X-ray crystallography (ORTEP of the synthesized compounds, **4b** and **4e**.

These substituted spirooxindoles were synthesized (*via* 1,3-dipolarcycloaddition reaction). Their anticancer activities against colon cancer (HCT-116), hepatocellular carcinoma (HepG2), and prostate cancer cell lines were evaluated. The selectivity of the active compounds towards the cancer cells versus the normal cells was also determined. The anticancer activity and their mechanism of action was further evaluated and the transactivation of p53 was confirmed. The designed compounds were docked against a co-crystalized structure of the standard p53-MDM2 inhibitor in order to understand their mode of action.

2. Results and discussion

2.1. Synthesis of 4a-p

The manuscript involved the design and synthesis of substituted spirooxindoles as potent MDM2 inhibitors, using an efficient 1,3-dipolar cycloaddition reaction [42]. The one-pot multi component reaction of *α,β*-unsaturated dienone derivative **1**, with the dicarbonyl compound **2** (substituted isatin), and amino acid derivative **3** (L-4-thiazolidinecarboxylic acid), was heated up in MeOH at 60 °C for 1.5–2.0 h to generate the focused cycloadduct library, **4a-p**, having 4 stereogeneric centers, in good to excellent yield (69–89%) (Scheme 1). The molecular complexity of the cycloadducts was assigned with different sets of spectroscopic techniques, including nuclear magnetic resonance (NMR) spectroscopic analyses including infrared (IR) spectroscopy, elemental analysis, ^{1}H NMR, ^{13}C NMR, mass spectrometry (MS), and X-ray crystallography. Interestingly, all the reactions revealed the cycloadduct, **4a-p,** as a single regioisomer with full chemoselectivity and diastereoselectivity (Fig. 2).

2.2. Docking study

A library of reportedly active spirooxindoles [43] and our synthesized compound, **4d**, was designed and energy was minimized using MMFF94 force field calculations. The MDM2 (PDB code: 5law [42,44]) catalytic domain was prepared for docking using Open Eye® software. Open Eye Omega application [45] was used to generate different conformations for each ligand. Docking was conducted using Fred [46] and the data was visualized using the Veda application. This software package generates consensus scoring, which is a filtering process, to obtain the virtual binding affinity, lower consensus score, and better binding affinity of the ligands towards the receptor. The study revealed that the standard spirooxindole, **6SJ**, interacts in the hydrophobic cleft with a consensus score of 41 via the formation of two hydrogen bonds (HB) coming from the NH of the indole moiety and oxygen of the hydroxyl group with Leu 54 (1.64 Å) and with Lys 94 (2.00 Å) respectively, Fig. 3A. Compound **4d** docked with MDM2, with a consensus score of 91, through a hydrophobic-hydrophobic interaction towards the p53-binding site in MDM2, without formation of HB (Fig. 3B). Interestingly, its docking pose showed the molecule as two-cleft; the styryl moiety (2,4 dichloro subs.) and oxindole scaffold are located in the right motif of the receptor, while aryl and thiazolo-pyrrolidine moieties adopted the left side of receptor. Despite this, compound **4d** overlaid with standard ligand **6SJ** and other reported compounds (Fig. 3C and D) [15,22,43]. Comparing compound **4d** with its analog **4e** showed dissimilarity, especially in the positions of important oxindole scaffolds (supplementary data; Fig. S50 and S51). This finding

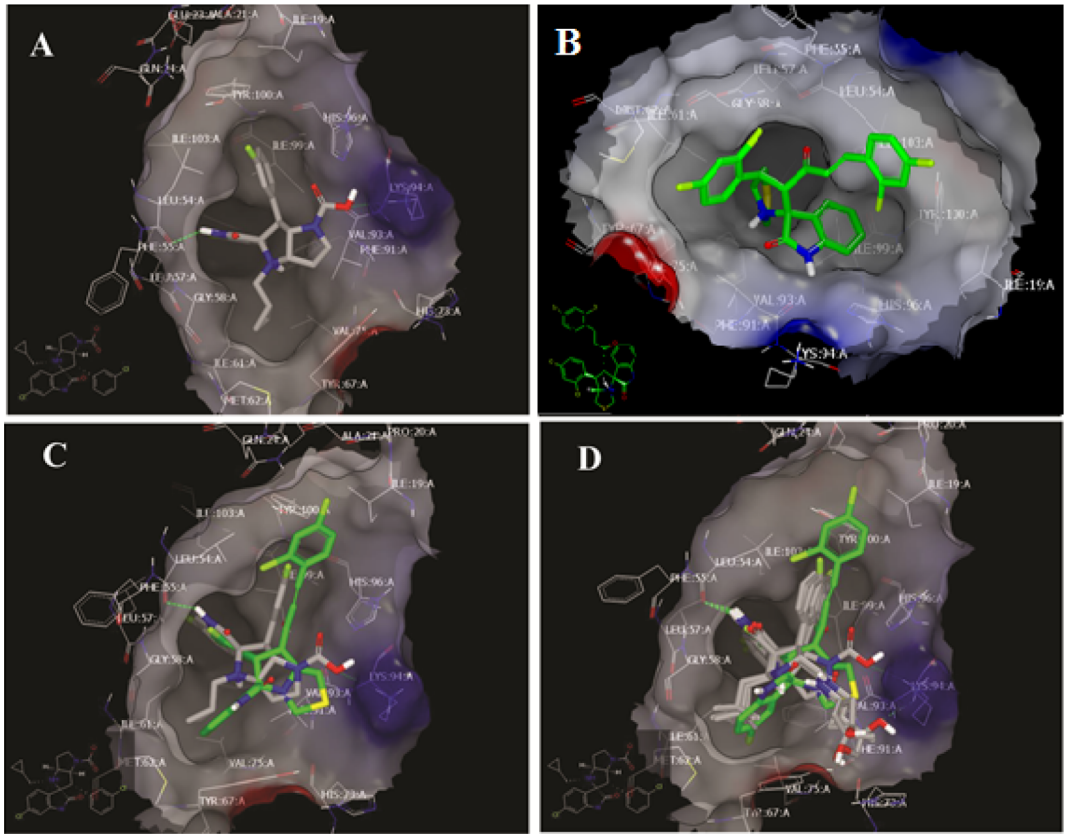

Fig. 3. Visual representation of standard **6SJ** docked with 5law, **(A)** showing HB interaction (green dotted line) as shown by Vida. **(B)** Visual representation of **4d** docked with 5law, showing hydrophobic-hydrophobic interaction. **(C)** Visual representation of **4d** (green color) superposed with standard **6SJ** and docked with 5law, showing hydrophobic-hydrophobic interaction. **(D)** Visual representation of **4d** (green color) overlaid with reported MDM inhibitors and docked with 5law.

Table 1
The cytotoxic activity of the synthesized compounds against colon cancer (HCT-116), hepatocellular carcinoma (HepG2) and prostate cancer cell lines. SI: selectivity index, STD: standard chemotherapeutic drug.

	Code	Cell line						
	4a-p	HCT-116		HepG2		PC-3		VERO-B
		μM	SI	μM	SI	μM	SI	μM
1	**4a**	9 ± 1	0.9	3.85 ± 0.3	**2.1**	> 50		8 ± 0.5
2	**4b**	8 ± 1.2	1.5	3.57 ± 0.5	**3.31**	> 50		11.8 ± 1
3	**4c**	3 ± 0.5	**2.3**	2.0 ± 0.5	**3.5**	2.7 ± 0.4	**2.6**	7 ± 0.45
4	**4d**	2 ± 0.6	**3.6**	0.85 ± 0.2	**5.9**	1.8 ± 0.3	**2.8**	5 ± 0.245
5	**4e**	3 ± 0.3	1	1.0 ± 0.3	**3**	> 50		3 ± 0.5
6	**4f**	3 ± 0.5	1	0.8 ± 0.1	**3.8**	> 50		3 ± 0.32
7	**4g**	2.5 ± 0.2	1	> 50		> 50		2.5 ± 0.2
8	**4h**	7 ± 0.9	1.1	2.25 ± 0.2	**3.3**	> 50		7.5 ± 0.6
9	**4i**	8 ± 0.3	0.9	2.4 ± 1.0	**2.9**	2.9 ± 0.2	**2.4**	7 ± 0.28
10	**4j**	14.5 ± 1.5	1.2	> 50		> 50		18 ± 2
11	**4k**	19 ± 2	1.3	> 50		> 50		25 ± 2.5
12	**4l**	1.57 ± 0.3	1.9	0.9 ± 0.1	**3.3**	1.5 ± 0.5	**2**	3 ± 0.56
13	**4m**	5 ± 0.3	1.2	2.4 ± 0.4	**2.5**	2.5 ± 0.2	**2.4**	6 ± 0.7
14	**4n**	2.9 ± 0.4	0.9	0.9 ± 0.2	**2.8**	1.0 ± 0.2	**2.5**	2.5 ± 0.12
15	**4o**	7 ± 0.6	1.1	2 ± 0.4	**4**	2.5 ± 0.5	**3.3**	8 ± 0.78
16	**4p**	3.5 ± 0.3	0.9	0.8 ± 0.1	**3.8**	1.5 ± 0.1	**2**	3 ± 0.35
STD	**cisplatin**	12.6 ± 2	0.4	5.5 ± 1	0.9	5.0 ± 0.5	1	5 ± 0.2

suggested that the presence of substituted cinnamoyl fragments namely 2,4-dichlorostyryl moiety acts as an arm and we can speculate it as an important new pharmacophore.

2.3. In vitro biological activity evaluation

The anticancer activity of the synthesized compounds (16 compounds) was tested against different cancer cells (HCT-116, PC-3 and HepG-2). The data showed that the 16 compounds (Table 1) possessed anticancer activity against colon cancer while 13 compounds was active against HepG-2 (Table 1) and only 8 compounds (Table 1) were active against prostate cancer, compared to the standard chemotherapeutic drug, cisplatin. All active compounds showed IC50 lower than 10 μM, except **4j** and **4 k** with colon cancer cells.

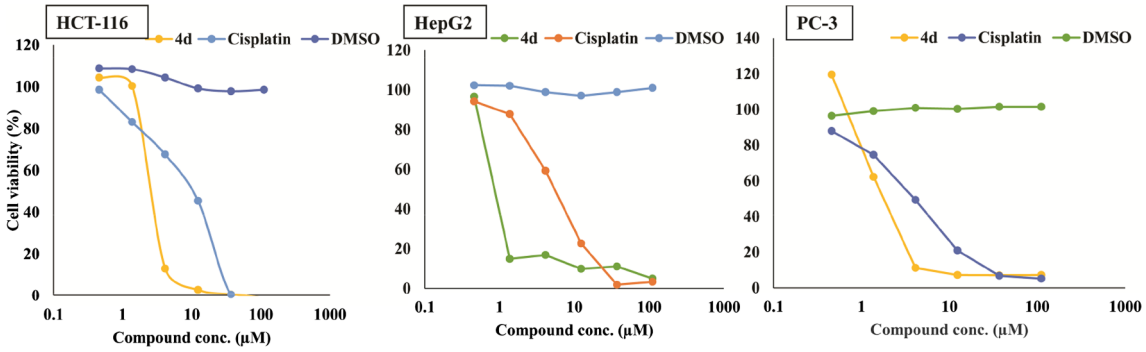

Fig. 4. Cytotoxic activity against different mammalian cancer cells. The colon cancer (HCT-116), hepatocellular carcinoma (HepG-2) or prostate cancer (PC-3) cells were treated with different concentrations of compound **4d**, cisplatin or DMSO. Cell viability was determined, after 48 h incubation, by MTT assay.

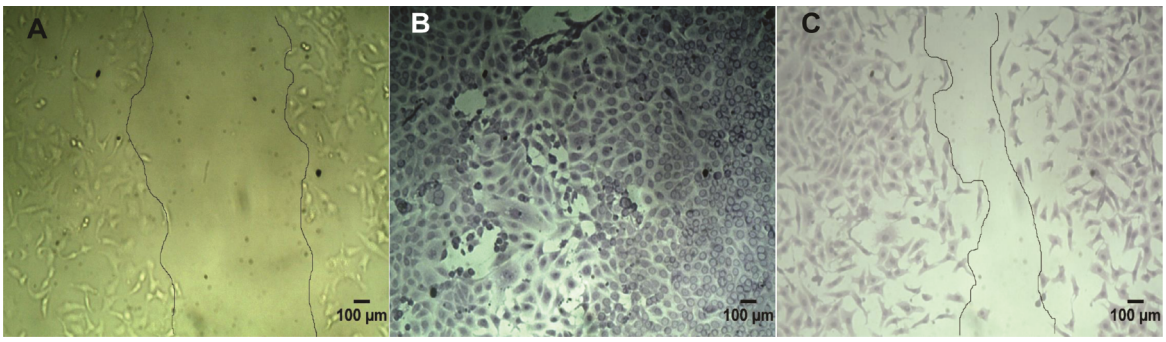

Fig. 5. Inhibition of wound healing by compound **4d**. Colon cancer cells (HCT-116) were treated with DMSO (A, B) or with 1 μM of compound **4d** (C). The photos for the wound was taken at (A) zero time (brightfield) or after 20 h of incubation (B, C) (crystal violet stained cells). After that, the cells were fixed with ice-cold methanol and stained with crystal violet. The untreated cells were able to close the wound and decrease the space between each other (B) while compound **4d** inhibited closing of the wound (C).

The active compounds against HepG2 or PC-3, were highly active with IC50 less than or equal to 0.5 μM in comparison to cisplatin. The selectivity of the active compound towards the cancer cells versus the normal cells was further studied by testing their antigrowth activity to the epithelial cells from the African green monkey (Vero-B). The selectivity index (SI) of the compounds were calculated as described in the supporting information. Out of the 16 active, anti-colon cancer compounds, only compounds **4c** and **4d** were highly selective (SI > 2) (HCT-116) (Table 1). On the other hand, the 13 active compounds against hepatocellular carcinoma showed SI higher than 2 (Table 1). The selectivity index of the active compounds against prostate cancer was greater than 2 as well (Table 1). The cytotoxicity of compound **4d** was further evaluated against the normal human lung fibroblast cells (WI-38) and the compound caused 40% cell death at 5 μM ± 0.54, which indicates the safety of the compound at 2 μM. This finding encouraged further analysis and study on the compound **4d**.

For the compounds listed in table 1, chemical structure–activity studies (SAR) showed that electron withdrawing group (EWG) substituents at styryl moieties are essential for potent *in vitro* activities. Also, these compounds (with EWG) exhibited higher potency against colon cancer cell line (4–8.5 fold to standard cisplatin, Table 1) more than HePG2 (2.5–6 folds to standard cisplatin, Table 1) and prostate cancers (1.8–5 folds to standard cisplatin, Table 1).

The presence of EWG linked to the styryl moiety of compound **4 g** (in case of HCT-116 cancer cell line), and halides as compounds **4d**, **4 l**, **4n**, **4c**, **4e** and **4f** (among all selected cancer cell lines), improved the activities of the compounds better than the unsubstituted analogs or those with electron donating groups (EDG) (**4a**, **4b**, and **4 h**) or with naphthyl rings (**4i**). Replacement of the phenyl group in the styryl moiety with the hetero groups, furyl or thiophenyl (**4 k**, and **4j** respectively) decreased the activity dramatically. For halide substitutions, Cl, Br and F substitutions, in that order, were the most favorable for compounds **4c**, **4f** and **4 m,** respectively. It is reasonable that the fluoro substitution was the least active as it is considered as a hydrogen isostere (unsubstituted). Taking into consideration the site of substitution, data revealed that *meta* substitution was better than *para* analogs e.g. **4 l** displayed two-fold higher activity than **4f** (in the case of HCT-116 cancer cell line, Table 1). Moreover, 2,4-dicholro substitution in **4d** resulted in two-fold higher activity than the corresponding positional isomer 2,6-dicholro substitution **4e**. The effect of the substitution on the indole ring showed that the presence of the bromo- atom linked at position 4 resulted in better activities than the corresponding chloro- and unsubstituted analogs for compounds **4p**, **4 m** and **4o**, respectively. Based on these findings and utilizing the docking visualization of target compounds, we can conclude that the site and type of substitution on styryl groups affect both the geometry of styryl moiety and the electrostatic similarity between molecules, thereby affecting compounds laying and interaction inside the receptor.

In this study, the broad spectrum active compound **4d** (Fig. 4) was used for further analysis because its IC50 was less than 4 μg/ml and its selectivity index for the cancer cells was greater than 2 [39]. The effect of compound **4d** on colony formation from a single colon cancer cell was evaluated by incubating the cells with 1 μM. Compound **4d** was able to better inhibit colony formation in comparison to the control (Figure S52, S53 and S54). Moreover, compound **4d** was able to stop cell migration and prevent wound healing (Fig. 6, Fig. S55). These results confirm the ability of compound **4d** to enhance tumor suppression (see Fig. 5).

Cell cycle analysis after treating colon cancer cells with 2 μM of compound **4d** revealed that the compound arrested around 34.5% and 15.5% of cells in G2/M and subG1, respectively (Figure A). The arrest of the cell cycle in subG1 indicated the induction of apoptosis, so the level of apoptotic cells either in early (+ve Annexin-V and −ve PI) or late stage (+ve Annexin-V and +ve PI) was determined by flow

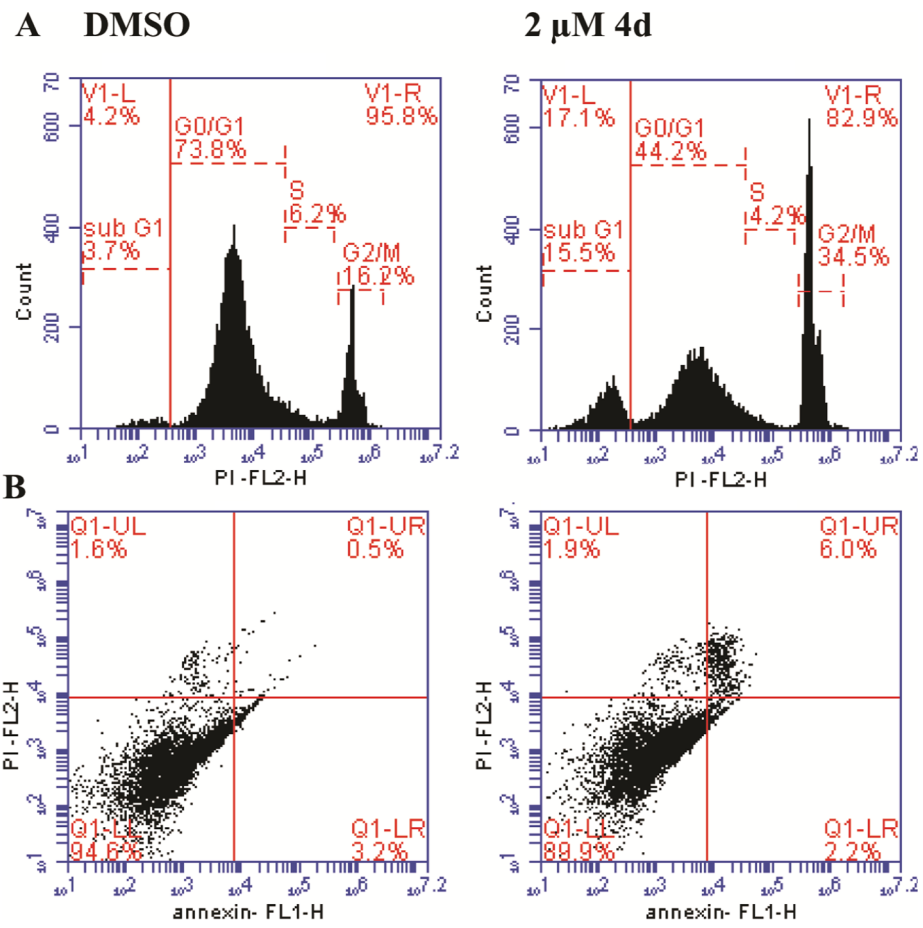

Fig. 6. (A) Compound **4d** (2 µM for 24 h) arrested colon cancer cells (HCT-116) at G2/M phase (34.5% of cell population), and induced apoptosis which is clear in the accumulation of around 15.5% of cells in subG1. The cells were incubated with or without 2 µM **4d** for 24 h. (B) Compound **4d** (2 µM) induced apoptosis after 48 h of incubation and around 2.2% of cells were in the early stage of apoptosis (lower right quadrant) and 6% of cells were in the late stage of apoptosis (upper right quadrant). The graphs represent one of two repeated experiments.

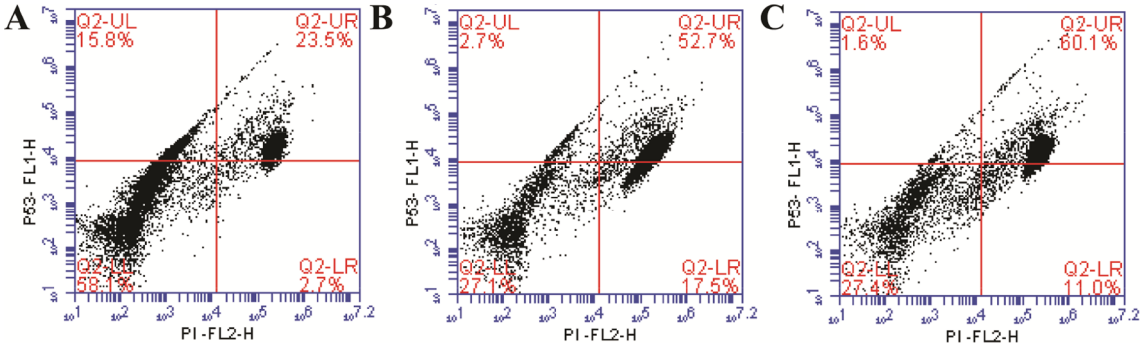

Fig. 7. Transactivation of p53 by compound **4d**. The HCT-116 cells were treated either with 1 µM (B) or 2 µM (C) for 48 h then collected, fixed and permeabilized. The permeabilized cells were stained with anti-p53 antibody and DNA-binding PI stain. About 23% of untreated cells showed a shift in fluorescence (A) (positive p53 and PI-stain) while the treated cells, either with 1 µM (B) or 2 µM (C), showed a significant increase in the number of stained cells (52.7% or 60.1%, respectively) confirming the activation of p53. The graphs represent one of two repeated experiments.

cytometry. Compound **4d** (2 µM), after 48 h treatment, greatly increased the apoptotic cells as depicted in (Fig. 7B). Since the 2-day treatment did not show cells in the early stage of apoptosis, we repeated the experiment with a shorter treatment time (24 h) and 1 µM of compound **4d**. We found that, even short time treatment and lower concentration could induce apoptosis (Supplementary information; Fig. S56).

2.3.1. Validation of inhibition of p53-MDM2 interaction

Molecular docking study showed that compound **4d** interacts in the hydrophobic cleft of MDM2 which is required for p53 binding. Compound **4d** binds with p53 and Phe 19, Trp 23 and Leu 26 residues in the MDM2 hydrophobic pocket at the *N*-terminal, where the DNA transactivation domain is localized [47,48]. However, p53 can bind with MDM2 at other positions within 120 amino terminal in MDM2. Nutlin, AMG232 [18] and MI-773 are small non-peptide molecules that disrupt p53 interaction with MDM2 via binding with the hydrophobic cleft of MDM2, leading to the accumulation of activated p53 [6,49–51].

In order to confirm the effect of compound **4d** on p53 activation, we incubated colon cancer cells with 2 µM of the compound and after 24 h, the cells were stained with antibody against p53 and analyzed by flow cytometry. We observed a significant increase in cells (60.1% ± 2 vs 23.5% ± 1.5 in untreated cells) that were positive for p53 and propidium iodide (nucleic acid stain) (Fig. 7).

Inhibition of p53-MDM2 interaction leads to inhibition of p53 ubiquitination and proteasomal degradation. The accumulated p53 is

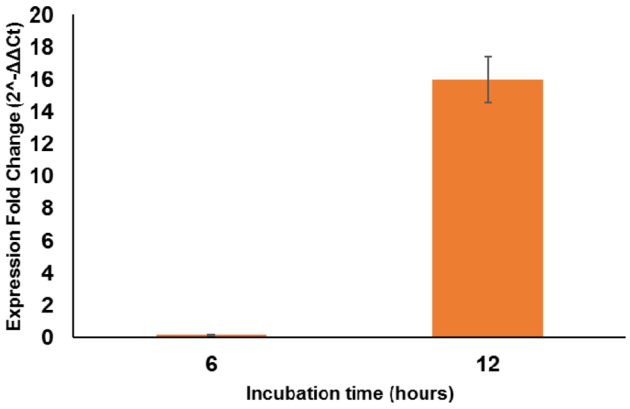

Fig. 8. Activation of p53 by compound **4d** induced the expression of the cell cycle inhibitor $P21^{cip1/WAF1}$ gene. The HCT-116 cells were treated by compound **4d** at 2 μM at the indicated time points followed by RNA extraction. The cDNA of $P21^{cip1/WAF1}$ was synthesized using specific primers, then normalized to the expression level of *GAPDH* as a reference gene. The error bar represents the standard deviation of results from two independent experiments.

translocated to the nucleus where it binds to specific DNA sequences for target genes involved in DNA repair. Additionally, transactivated p53 leads to apoptosis and growth arrest in cells with unrepairable DNA damage [9,10,14]. Based on the observations above, the expression level of the cell cycle inhibitor, p21, in the treated cells was evaluated by quantitative RT-PCR. The analysis confirmed p53 activation leading to an increase in mRNA levels of the $P21^{cip1/WAF1}$ gene, peaking after 12 h, then decreasing after 24 h, indicating translation to p21 inhibitor protein (Fig. 8). Upon expression of p21, cell growth was halted and apoptosis was initiated. *P*21 inhibits the cell cycle via two pathways; by inhibiting the kinase activity of cyclin-dependent kinase (CDK), and preventing the binding of proliferating cell nuclear antigen (PCNA) to DNA polymerase, leading to inhibition of DNA synthesis [52].

P53 regulates the apoptotic process at multiple points, intrinsic or extrinsic pathways, in order to increase the ratio of proapoptotic: antiapoptotic proteins. The main target genes for p53, are Bcl2 family genes such as Bax. Bax binds to the mitochondrial membrane, leading to its permeabilization and the release of cytochrome *c*, where it forms a complex with Apaf-1 and caspase-9, leading to the cleavage of procaspase-9 [53–56]. Cleaved caspase-9 in turn activates caspase 3, the hallmark of apoptosis [57,58]. Therefore, the level of proapoptotic and apoptotic proteins that are regulated by transactivated p53 was measured by flow cytometry [54]. In this study, treatment of colon cancer cells with compound **4d** led to a decrease in the level of antiapoptotic protein, Bcl2 (16.0% ± 0.4 vs 24.6% ± 2 in untreated cells), and an increase in proapoptotic Bax protein (15.3% ± 1 vs 4.5% ± 0.65 in untreated cells) (Fig. 9). Further analysis was performed to evaluate the level of activated caspase-9 in cells treated with compound **4d**. The results revealed that compound **4d** treatment led to an increase in the level of caspase-9 (25.8% ± 2 vs 10.6% ± 0.5 in untreated cells) (Fig. 10). Once the effector caspase-9 is activated, it leads to the activation of the executioner caspase-3. Indeed, treatment of colon cancer cells with compound **4d** led to increased caspase-3 levels (74.4% ± 4 vs 50.6% ± 2 in untreated cells) (Fig. 10), which further indicates the cytotoxic activity against colon cancer and induction of apoptosis by compound **4d**.

Apoptosis can be induced via two pathways, the mitochondrial (intrinsic pathway) [56] and extrinsic pathways [59]. We further analyzed the possible induction of the extrinsic apoptotic pathway by treatment with compound **4d**. As shown in Fig. 10, compound **4d** increased the level of caspase-8 as well in treated colon cancer cells in comparison to the control (31.2% ± 2.5 vs 14.5% ± 1). A link was found between activated p53 and increased gene expression of extrinsic apoptotic proteins (*Fas/CD95* [44], *DR5* [60] and Fas ligand [61]).

Here, we present a new potential p53-MDM2 inhibitor which is able to activate p53. The activated p53 led to colony formation and cell migration. Inhibition for the two pathways of metastasis could be via the down regulation of metalloproteinases (such as MMP-1, MMP-2 and MMP-9) by the activated p53. It has been reported that the over expression of wild-type p53 in colon cancer cells led to the down regulation of MMP-1 [3], MMP-2 and MMP-9 [62] which inhibited colony formation in soft agar [63,64]. The new potential spirooxindole derivative (compound **4d**) was also able to induce both intrinsic and extrinsic apoptotic pathways. These results present a new lead compound that is worth further preclinical studies (*in vivo*).

3. Conclusion

In this study, a newly synthesized spirooxindole, **4d**, was able to activate p53 and restore its function, which was demonstrated by wound healing inhibition and colony formation. The transactivation of p53 by compound **4d** was confirmed by the increase in *p21* gene transcription in treated cells. p53 regulates apoptosis at multiple points, through intrinsic or extrinsic pathways, in order to increase the ratio of

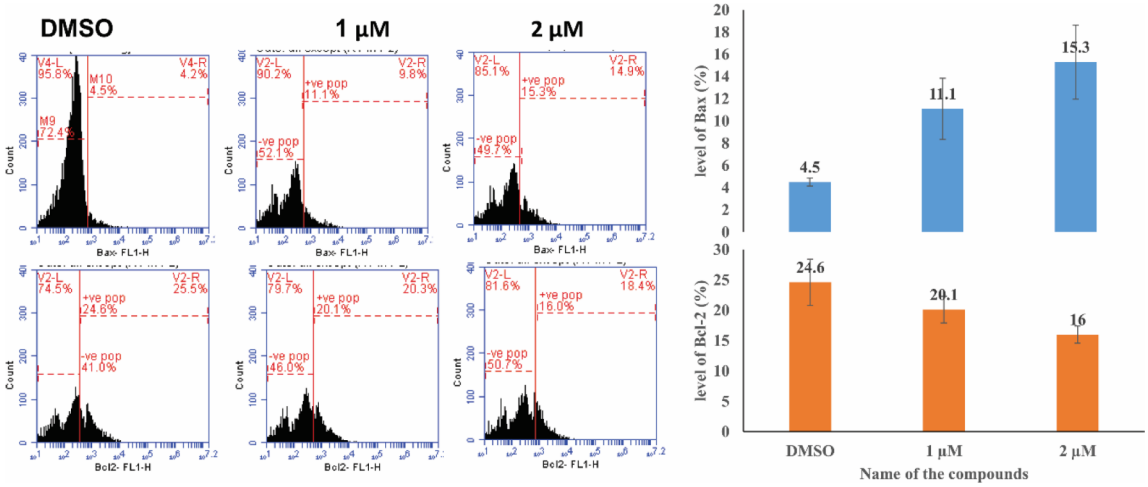

Fig. 9. Compound **4d** induced apoptosis via an increase in Bax, and a decrease in the level of the antiapoptotic protein, Bcl-2. The HCT-116 cells were treated with the indicated concentrations of compound 4d for 48 h then proceed for the detection of pro- (Bax) or anti-apoptotic (Bcl-2) protein levels. − ve pop and + ve pop are negative and positive cell populations, respectively, for the marker under analysis. The error bar represents the standard deviation of two repeated experiments. The numbers in the bar graph represent one of the experiments.

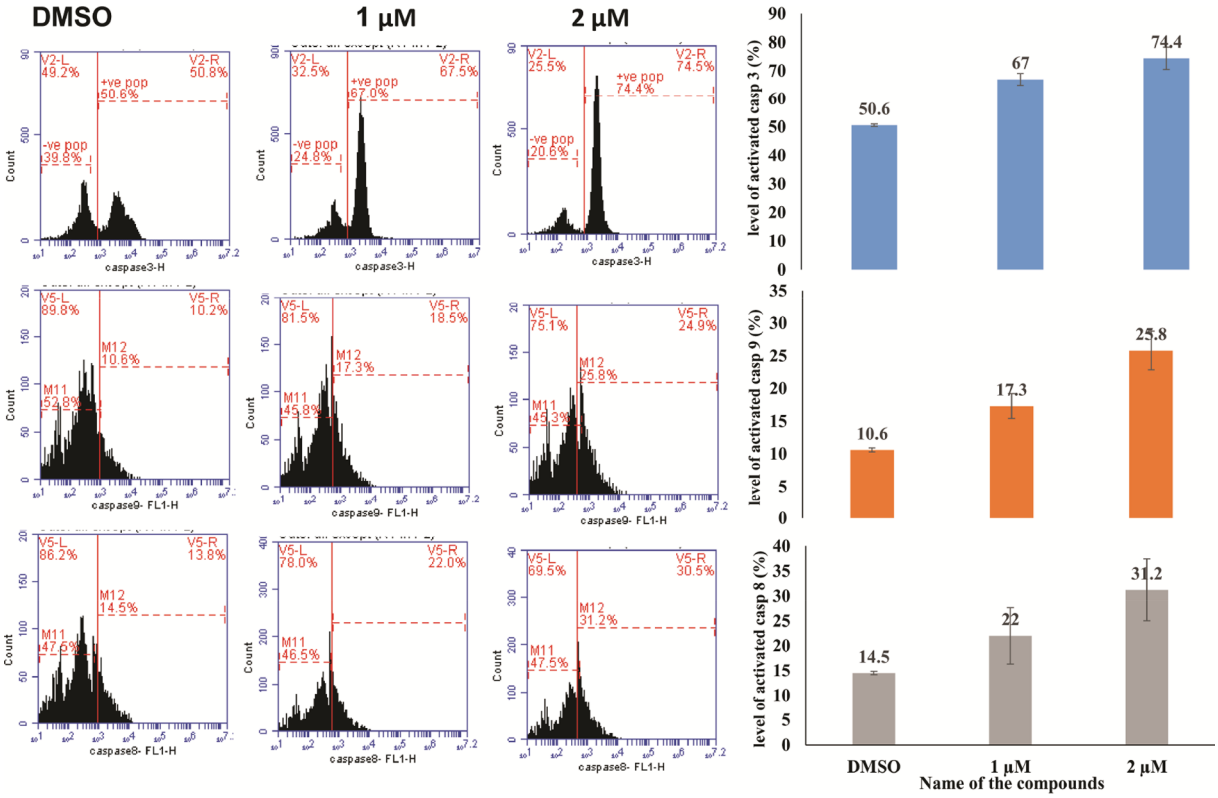

Fig. 10. Compound **4d** induced apoptosis through mitochondrial and death receptor pathways. −ve pop (M11) and +ve pop (M12) are negative and positive cell populations, respectively, for the marker under analysis. The HCT-116 cells were treated with the indicated concentrations of compound 4d for 48 h then processed for the detection of executioner caspase 3 or the activators caspase 9 and 8 levels. The error bar represents the standard deviation of two repeated experiments. The numbers in the bar graph represent one of the experiments.

proapoptotic: antiapoptotic proteins. The main target genes for p53 are Bcl2 family genes, such as Bax. Compound **4d** was able to inhibit the binding of p53 with MDM2 leading to an increase in the level of intrinsic effectors, such as Bax and caspase-9. Moreover, compound **4d** activated the extrinsic apoptotic pathway. The obtained results are compelling evidence of the ability of our newly synthesized spirooxindoles to inhibit the interaction between the tumor suppressor, p53, and MDM2 and requires further mechanistic *in vivo* studies. Judging from the docking study, the installation of a multiple fused-ring system containing styryl (or benzylidine) part allowed the precise positioning of functional groups for $\pi - \pi$ interactions. The data obtained suggests the need for further metabolic profiling of the new lead compound **4d**.

4. Experimental

The general procedure for the synthesis of the designed compounds as well as full characterization are discussed in the supplementary information [66].

4.1. Docking studies

This was done using OpenEye molecular Modeling software. Complete details are reported in the supplementary information [28,29,37–39,58,59].

4.2. In vitro cytotoxic activity

All assay procedures including cytotoxicity; Selectivity index (SI) calculations; Colony forming assay; Wound healing assay; Cell cycle analysis; Induction of apoptosis; Determination of p53 level and apoptotic markers; qRT-PCR for detection of p21 gene expression are reported in the supplementary information [40–42,65].

Author contributions

AB designed the project; MSI and HMG synthesized the target compounds; AMA assisted with data analysis; FFE designed, performed and wrote the biological activities. YE performed and wrote the molecular docking; HAG carried out the X-ray single crystal structural studies; AB and FB supervised, revised and approved the work for submission. All authors approved the final version of the manuscript.

Acknowledgements

The authors would like to extend their sincere appreciation to the Deanship of Scientific Research at King Saud University for providing funding to the research group No. (RGP-257). The authors would like to thank RSSU at KSU for the editing and reviewing the English language of the manuscript.

Appendix A. Supplementary material

Supplementary data to this article can be found online at https://doi.org/10.1016/j.bioorg.2019.01.053.

References

[1] R.L. Siegel, K.D. Miller, A. Jemal, Cancer statistics, 2018, CA: A Cancer J. Clinicians 68 (1) (2018) 7–30.
[2] G. Szakács, J.K. Paterson, J.A. Ludwig, C. Booth-Genthe, M.M. Gottesman, Targeting multidrug resistance in cancer, Nat. Rev. Drug Discovery 5 (3) (2006) 219.
[3] Y. Sun, Y. Sun, L. Wenger, J.L. Rutter, C.E. Brinckerhoff, H.S. Cheung, p53 down-regulates human matrix metalloproteinase-1 (Collagenase-1) gene expression, J. Biol. Chem. 274 (17) (1999) 11535–11540.
[4] J.M. Cummins, C. Rago, M. Kohli, K.W. Kinzler, C. Lengauer, B. Vogelstein, Tumour suppression: disruption of HAUSP gene stabilizes p53, Nature 428 (2004) 6982.

[5] R.D. Everett, M. Meredith, A. Orr, A. Cross, M. Kathoria, J. Parkinson, A novel ubiquitin-specific protease is dynamically associated with the PML nuclear domain and binds to a herpesvirus regulatory protein, The EMBO J. 16 (3) (1997) 566–577.
[6] G. Liao, D. Yang, L. Ma, W. Li, L. Hu, L. Zeng, P. Wu, L. Duan, Z. Liu, The development of piperidinones as potent MDM2-P53 protein-protein interaction inhibitors for cancer therapy, Eur. J. Med. Chem. 159 (2018) 1–9.
[7] F. Bartel, A. Meye, P. Würl, M. Kappler, M. Bache, C. Lautenschläger, U. Grünbaum, H. Schmidt, H. Taubert, Amplification of the MDM2 gene, but not expression of splice variants of MDM2 MRNA, is associated with prognosis in soft tissue sarcoma, Int. J. Cancer 95 (3) (2001) 168–175.
[8] Y.F. Ramos, R. Stad, J. Attema, L.T. Peltenburg, A.J. van der Eb, A.G. Jochemsen, Aberrant expression of HDMX proteins in tumor cells correlates with wild-type p53, Cancer Res. 61 (5) (2001) 1839–1842.
[9] G.L. Bond, W. Hu, A.J. Levine, MDM2 is a central node in the p53 pathway: 12 years and counting, Curr. Cancer Drug Targets 5 (1) (2005) 3–8.
[10] M. Wade, Y.V. Wang, G.M. Wahl, The p53 orchestra: Mdm2 and Mdmx set the tone, Trends Cell Biol. 20 (5) (2010) 299–309.
[11] C.E. Bueso-Ramos, Y. Yang, P. McCown, S. Stass, M. Albitar, The human MDM-2 oncogene is overexpressed in leukemias, Blood 82 (9) (1993) 2617–2623.
[12] B. Yu, D.-Q. Yu, H.-M. Liu, Spirooxindoles: Promising scaffolds for anticancer agents, Eur. J. Med. Chem. 97 (2015) 673–698.
[13] S. Shangary, K. Ding, S. Qiu, Z. Nikolovska-Coleska, J.A. Bauer, M. Liu, G. Wang, Y. Lu, D. McEachern, D. Bernard, Reactivation of p53 by a specific MDM2 antagonist (MI-43) leads to p21-mediated cell cycle arrest and selective cell death in colon cancer, Mol. Cancer Ther. 7 (6) (2008) 1533–1542.
[14] P.H. Kussie, S. Gorina, V. Marechal, B. Elenbaas, J. Moreau, A.J. Levine, N.P. Pavletich, Structure of the MDM2 oncoprotein bound to the p53 tumor suppressor transactivation domain, Science 274 (5289) (1996) 948–953.
[15] Q. Ding, Z. Zhang, J.-J. Liu, N. Jiang, J. Zhang, T.M. Ross, X.-J. Chu, D. Bartkovitz, F. Podlaski, C. Janson, Discovery of RG7388, a potent and selective p53–MDM2 inhibitor in clinical development, J. Med. Chem. 56 (14) (2013) 5979–5983.
[16] A.Z. Gonzalez, J. Eksterowicz, M.D. Bartberger, H.P. Beck, J. Canon, A. Chen, D. Chow, J. Duquette, B.M. Fox, J. Fu, Selective and potent morpholinone inhibitors of the MDM2–p53 protein–protein interaction, J. Med. Chem. 57 (6) (2014) 2472–2488.
[17] A. Leoni, A. Locatelli, R. Morigi, M. Rambaldi, 2-Indolinone a versatile scaffold for treatment of cancer: a patent review (2008–2014), Expert Opin. Ther. Pat. 26 (2) (2016) 149–173.
[18] Y. Rew, D. Sun, Discovery of a small molecule MDM2 inhibitor (AMG 232) for treating cancer, J. Med. Chem. 57 (15) (2014) 6332–6341.
[19] S. Yu, D. Qin, S. Shangary, J. Chen, G. Wang, K. Ding, D. McEachern, S. Qiu, Z. Nikolovska-Coleska, R. Miller, Potent and orally active small-molecule inhibitors of the MDM2− p53 interaction, J. Med. Chem. 52 (24) (2009) 7970–7973.
[20] P. Chène, Inhibiting the p53–MDM2 interaction: an important target for cancer therapy, Nat. Rev. Cancer 3 (2) (2003) 102–109.
[21] X. Wu, J.H. Bayle, D. Olson, A.J. Levine, The p53-mdm-2 autoregulatory feedback loop, Genes Dev. 7 (7a) (1993) 1126–1132.
[22] Y. Zhao, S. Yu, W. Sun, L. Liu, J. Lu, D. McEachern, S. Shargary, D. Bernard, X. Li, T. Zhao, A potent small-molecule inhibitor of the MDM2–p53 interaction (MI-888) achieved complete and durable tumor regression in mice, J. Med. Chem. 56 (13) (2013) 5553–5561.
[23] C. Zhuang, Z. Miao, L. Zhu, G. Dong, Z. Guo, S. Wang, Y. Zhang, Y. Wu, J. Yao, C. Sheng, Discovery, synthesis, and biological evaluation of orally active pyrrolidone derivatives as novel inhibitors of p53–MDM2 protein–protein interaction, J. Med. Chem. 55 (22) (2012) 9630–9642.
[24] A.M. Sosin, A.M. Burger, A. Siddiqi, J. Abrams, R.M. Mohammad, A.M. Al-Katib, HDM2 antagonist MI-219 (spiro-oxindole), but not Nutlin-3 (cis-imidazoline), regulates p53 through enhanced HDM2 autoubiquitination and degradation in human malignant B-cell lymphomas, J. Hematol. Oncol. 5 (1) (2012) 57.
[25] M. Rottmann, C. McNamara, B.K. Yeung, M.C. Lee, B. Zou, B. Russell, P. Seitz, D.M. Plouffe, N.V. Dharia, J. Tan, Spiroindolones, a potent compound class for the treatment of malaria, Science 329 (5996) (2010) 1175–1180.
[26] L. Upton, P. Brock, T. Churcher, A. Ghani, P. Gething, M. Delves, K. Sala, D. Leroy, R. Sinden, A. Blagborough, Lead clinical and preclinical antimalarial drugs can significantly reduce sporozoite transmission to vertebrate populations, Antimicrob. Agents Chemother. 59 (1) (2015) 490–497.
[27] C.-B. Cui, H. Kakeya, H. Osada, Novel mammalian cell cycle inhibitors, spirotryprostatins A and B, produced by Aspergillus fumigatus, which inhibit mammalian cell cycle at G2/M phase, Tetrahedron 52 (39) (1996) 12651–12666.
[28] A.P. Antonchick, C. Gerding-Reimers, M. Catarinella, M. Schürmann, H. Preut, S. Ziegler, D. Rauh, H. Waldmann, Highly enantioselective synthesis and cellular evaluation of spirooxindoles inspired by natural products, Nat. Chem. 2 (9) (2010) 735–740.
[29] M.M. Lo, C.S. Neumann, S. Nagayama, E.O. Perlstein, S.L. Schreiber, A library of spirooxindoles based on a stereoselective three-component coupling reaction, J. Am. Chem. Soc. 126 (49) (2004) 16077–16086.
[30] M.M. Santos, Recent advances in the synthesis of biologically active spirooxindoles, Tetrahedron 52 (70) (2014) 9735–9757.
[31] G.M. Popowicz, A. Czarna, S. Wolf, K. Wang, W. Wang, A. Dömling, T.A. Holak, Structures of low molecular weight inhibitors bound to MDMX and MDM2 reveal new approaches for p53-MDMX/MDM2 antagonist drug discovery, Cell Cycle 9 (6) (2010) 1104–1111.
[32] K. Ding, Y. Lu, Z. Nikolovska-Coleska, G. Wang, S. Qiu, S. Shangary, W. Gao, D. Qin, J. Stuckey, K. Krajewski, Structure-based design of spiro-oxindoles as potent, specific small-molecule inhibitors of the MDM2−p53 interaction, J. Med. Chem. 49 (12) (2006) 3432–3435.
[33] W. Wang, Y. Hu, Small molecule agents targeting the p53-MDM2 pathway for cancer therapy, Med. Res. Rev. 32 (6) (2012) 1159–1196.
[34] G.J. Mei, F. Shi, Catalytic asymmetric synthesis of spirooxindoles: recent developments, Chem. Commun. 54 (2018) 6607–6621.
[35] J.A. Xiao, H.G. Zhang, S. Liang, J.W. Ren, H. Yang, X.Q. Chen, Synthesis of Pyrrolo (spiro-[2.3′]-oxindole)-spiro-[4.3 ″]-oxindole via 1, 3-Dipolar Cycloaddition of Azomethine Ylides with 3-Acetonylideneoxindole, J. Org. Chem. 78 (22) (2013) 11577–11583.
[36] Q. Xu, D. Wang, Y. Wei, M. Shi, Highly efficient and stereoselective construction of bispirooxindole derivatives via a three-component 1, 3-dipolar cycloaddition reaction, ChemistryOpen 3 (3) (2014) 93–98.
[37] W. Dai, H. Lu, X. Li, F. Shi, S.J. Tu, Diastereo-and enantioselective construction of a bispirooxindole scaffold containing a tetrahydro-β-carboline moiety through an organocatalytic asymmetric cascade reaction, Chem.–A Eur. J. 20 (36) (2014) 11382–11389.
[38] C.S. Wang, R.Y. Zhu, J. Zheng, F. Shi, S.J. Tu, Enantioselective construction of spiro [indoline-3, 2′-pyrrole] framework via catalytic asymmetric 1, 3-dipolar cycloadditions using allenes as equivalents of alkynes, J. Org. Chem. 80 (1) (2014) 512–520.
[39] W. Dai, X.L. Jiang, Q. Wu, F. Shi, S.J. Tu, Diastereo-and enantioselective construction of 3, 3′-pyrrolidinyldispirooxindole framework via catalytic asymmetric 1, 3-dipolar cycloadditions, J. Org. Chem. 80 (11) (2015) 5737–5744.
[40] Y.M. Wang, H.H. Zhang, C. Li, T. Fan, F. Shi, Catalytic asymmetric chemoselective 1, 3-dipolar cycloadditions of an azomethine ylide with isatin-derived imines: diastereo-and enantioselective construction of a spiro [imidazolidine-2, 3′-oxindole] framework, Chem. Commun. 52 (9) (2016) 1804–1807.
[41] C. Li, H. Lu, X.X. Sun, G.J. Mei, F. Shi, Diastereo-and enantioselective construction of spirooxindole scaffolds through a catalytic asymmetric [3+ 3] cycloaddition, Org. Biomol. Chem. 15 (22) (2017) 4794–4797.
[42] A. Gollner, D. Rudolph, H. Arnhof, M. Bauer, S.M. Blake, G. Boehmelt, X.-L. Cockroft, G. Dahmann, P. Ettmayer, T. Gerstberger, J. Karolyi-Oezguer, D. Kessler, C. Kofink, J. Ramharter, J. Rinnenthal, A. Savchenko, R. Schnitzer, H. Weinstabl, U. Weyer-Czernilofsky, T. Wunberg, D.B. McConnell, Discovery of Novel Spiro[3H-indole-3,2′-pyrrolidin]-2(1H)-one Compounds as Chemically Stable and Orally Active Inhibitors of the MDM2–p53 Interaction, J. Med. Chem. 59 (22) (2016) 10147–10162.
[43] A. Gollner, D. Rudolph, H. Arnhof, M. Bauer, S.M. Blake, G. Boehmelt, X.-L. Cockroft, G. Dahmann, P. Ettmayer, T. Gerstberger, Discovery of novel spiro [3 H-indole-3, 2′-pyrrolidin]-2 (1 H)-one compounds as chemically stable and orally active inhibitors of the MDM2–p53 interaction, J. Med. Chem. 59 (22) (2016) 10147–10162.
[44] L.B. Owen-Schaub, W. Zhang, J.C. Cusack, L.S. Angelo, S.M. Santee, T. Fujiwara, J.A. Roth, A.B. Deisseroth, W.-W. Zhang, E. Kruzel, Wild-type human p53 and a temperature-sensitive mutant induce Fas/APO-1 expression, Mol. Cell. Biol. 15 (6) (1995) 3032–3040.
[45] P.C. Hawkins, A.G. Skillman, G.L. Warren, B.A. Ellingson, M.T. Stahl, Conformer generation with OMEGA: algorithm and validation using high quality structures from the Protein Databank and Cambridge Structural Database, J. Chem. Inf. Model. 50 (4) (2010) 572–584.
[46] M. McGann, FRED pose prediction and virtual screening accuracy, J. Chem. Inf. Model. 51 (3) (2011) 578–596.
[47] K. Likhitwitayawuid, C.K. Angerhofer, H. Chai, J.M. Pezzuto, G.A. Cordell, N. Ruangrungsi, Cytotoxic and antimalarial alkaloids from the tubers of Stephania pierrei, J. Nat. Prod. 56 (9) (1993) 1468–1478.
[48] G.G. Dodson, D.P Lane, C. Verma, Molecular simulations of protein dynamics: New windows on mechanisms in biology, 2008, vol. 9, p 144–150.
[49] J. Huei Wong, M. Alfatah, M. Fang Sin, H. May Sim, C. Verma, D.P. Lane, P. Arumugam, A yeast two-hybrid system for the screening and characterization of small-molecule inhibitors of protein–protein interactions identifies a novel putative Mdm2-binding site in p53, BMC Biol. 15 (2017) 108.
[50] S. Wang, W. Sun, Y. Zhao, D. McEachern, I. Meaux, C. Barrière, J.A. Stuckey, J.L. Meagher, L. Bai, L. Liu, SAR405838: an optimized inhibitor of MDM2–p53 interaction that induces complete and durable tumor regression, Cancer Res. (2014).
[51] L.T. Vassilev, B.T. Vu, B. Graves, D. Carvajal, F. Podlaski, Z. Filipovic, N. Kong, U. Kammlott, C. Lukacs, C. Klein, In vivo activation of the p53 pathway by small-molecule antagonists of MDM2, Science 303 (5659) (2004) 844–848.
[52] S. Shangary, S. Wang, Small-molecule inhibitors of the MDM2-p53 protein-protein interaction to reactivate p53 function: a novel approach for cancer therapy, Annu. Rev. Pharmacol. Toxicol. 49 (2009) 223–241.
[53] T. Abbas, A. Dutta, p21 in cancer: intricate networks and multiple activities, Nat. Rev. Cancer 9 (6) (2009) 400–414.
[54] K. Nakano, K.H. Vousden, PUMA, a novel proapoptotic gene, is induced by p53, Mol. Cell 7 (3) (2001) 683–694.
[55] D. Wlodkowic, J. Skommer, Z. Darzynkiewicz, Flow cytometry-based apoptosis detection, Methods Mol. Biol. (Clifton, N.J.) 559 (2009), https://doi.org/10.1007/978-1-60327-017-5_2.
[56] J.D. Amaral, J.M. Xavier, C.J. Steer, C.M. Rodrigues, The role of p53 in apoptosis, Discovery Med. 9 (45) (2010) 145–152.
[57] M.S. Soengas, R. Alarcon, H. Yoshida, R. Hakem, T. Mak, S. Lowe, Apaf-1 and caspase-9 in p53-dependent apoptosis and tumor inhibition, Science 284 (5411) (1999) 156–159.
[58] J.S. Fridman, S.W. Lowe, Control of apoptosis by p53, Oncogene 22 (56) (2003) 9030.
[59] D. Twiddy, K. Cain, Caspase-9 cleavage, do you need it? Biochem. J. 405 (Pt 1) (2007) e1.

[60] D. Tang, J.M. Lahti, V.J. Kidd, Caspase-8 activation and bid cleavage contribute to MCF7 cellular execution in a caspase-3-dependent manner during staurosporine-mediated apoptosis, J. Biol. Chem. 275 (13) (2000) 9303–9307.
[61] G.S. Wu, T.F. Burns, E.R. McDonald, W. Jiang, R. Meng, I.D. Krantz, G. Kao, D.-D. Gan, J.-Y. Zhou, R. Muschel, KILLER/DR5 is a DNA damage–inducible p53–regulated death receptor gene, Nat. Genet. 17 (2) (1997) 141–143.
[62] H.L. Maecker, Z. Yun, H.T. Maecker, A.J. Giaccia, Epigenetic changes in tumor Fas levels determine immune escape and response to therapy, Cancer Cell 2 (2) (2002) 139–148.
[63] J. Liu, M. Zhan, J.A. Hannay, P. Das, S.V. Bolshakov, D. Kotilingam, D. Yu, A.F. Lazar, R.E. Pollock, D. Lev, Wild-type p53 inhibits nuclear factor-κB–induced matrix metalloproteinase-9 promoter activation: implications for soft tissue sarcoma growth and metastasis, Mol. Cancer Res. 4 (11) (2006) 803–810.
[64] S.J. Baker, S. Markowitz, E.R. Fearon, J. Willson, B. Vogelstein, Suppression of human colorectal carcinoma cell growth by wild-type p53, Science 249 (4971) (1990) 912–915.
[65] P.-L. Chen, Y. Chen, R. Bookstein, W.-H. Lee, Genetic mechanisms of tumor suppression by the human p53 gene, Science 250 (4987) (1990) 1576–1580.
[66] A. Barakat, M.S. Islam, A.M. Al Majid, H.M. Ghawas, F.F. El-Senduny, F.A. Badria, Y.A.M.M. Elshaier, H.A. Ghabbour, Substitute spirooxindoles, US9822128B1; Nov., 21, 2017.

Further reading

[67] M.S. Islam, H.M. Ghawas, F.F. El-Senduny, A. Al-majid, F.A. Badria, Y.A.M.M. Elshaier, A. Barakat, Synthesis of new thiazolo-pyrrolidine /Spirooxindole tethered to 3-acylindole as anticancer agents, Bioorg. Chem. 82 (2019) 423–430.